Zhou et al. EURASIP Journal on Advances in Signal Processing (2019) 2019:13
https://doi.org/10.1186/s13634-019-0610-z

EURASIP Journal on Advances in Signal Processing

RESEARCH Open Access

# A fast STAP method using persymmetry covariance matrix estimation for clutter suppression in airborne MIMO radar

Yan Zhou, Xiaoxuan Chen*, Yanyan Li, Lin Wang, Bo Jiang and Dingyi Fang

## Abstract

In general, the space-time adaptive processing (STAP) can achieve excellent clutter suppression and moving target detection performance in the airborne multiple-input multiple-output (MIMO) radar for the increasing system degrees of freedom (DoFs). However, the performance improvement is accompanied by a dramatic increase in computational cost and training sample requirement. As one of the most efficient dimension-reduced STAP methods, the extended factored approach (EFA) transforms the full-dimension STAP problem into several small-scale adaptive processing problems, and therefore alleviates the computational cost and training sample requirement. However, it cannot effectively work in the airborne MIMO radar since sufficient training samples are unavailable. Aiming at the problem, a fast iterative method using persymmetry covariance matrix estimation in the airborne MIMO radar is proposed. In this method, the clutter covariance matrix is estimated by the original data and the constructed data. Then, the spatial weight vector in EFA is decomposed into the Kronecker product of two short-weight vectors. The bi-iterative algorithm is exploited to obtain the desired weight vectors. Simulation results demonstrate the effectiveness of our proposed method.

**Keywords:** Multiple-input multiple-output (MIMO) radar, Space-time adaptive processing (STAP), Clutter suppression, Bi-iterative

## 1 Introduction

Since the concept of multiple-input multiple-output (MIMO) radar was first proposed in [1], it has been receiving considerable attention for its superiority in spatial diversity and available degrees of freedom (DoFs) compared with its single-input multiple-output (SIMO) counterpart [1–4]. More recently, the researches on the airborne MIMO radar have been extended to the space-time adaptive processing (STAP) [5–8], which is an important technique in airborne radars due to the remarkable ability of clutter suppression that facilitates the downstream signal processing tasks suffering from high clutter rates such as multi-target detecting and tracking [9–11].

By far, a number of literatures have studied various STAP methods in the airborne MIMO radar. Many existing STAP methods that were once studied in the airborne SIMO radar are also applied into the airborne MIMO radar and show superior performance with sufficient homogeneous training sample support [12–33]. The dimension-reduced STAP methods [12–18], such as joint domain localized (JDL) [13], generalized multiple beams (GMB) [14], and pulse repetition interval (PRI)-staggered algorithm [15], can reduce the adaptive dimension and hence reduce the computational cost and the number of required training samples. However, they are either computational intensive or sensitive to amplitude and phase errors. On the other hand, the rank-reduced STAP methods [8, 19–22], such as principle components (PC) [19] and cross-spectrum method (CSM) [20], make the eigendecomposition to the clutter covariance matrix (CCM) and try to estimate the clutter subspace. Although the rank-reduced STAP methods exploit the low rank property of clutter and reduce the number of required training samples to twice of the clutter rank, they are computational intensive due to the CCM eigendecomposition. Besides, the eigenvectors of CCM cannot be accurately estimated when the number of training samples is inadequate. Knowledge-aided (KA)

* Correspondence: chenxx@nwu.edu.cn
School of Information Science and Technology, Northwest University, Xi'an 710127, China

radar, which can use the a priori knowledge such as the digital elevation map (DEM) and geospatial databases to enhance STAP performance with small training samples support, has been attracting increasing attentions of researchers and practitioners [23–27]. However, the precise information of the a priori knowledge is hard to obtain. More recently, based on the sparsity of clutter distribution on spatial-temporal plane, the sparse recovery STAP interests many researchers for the very few training samples demanding. On the one hand, the sparse recovery STAP is accomplished by constructing the overcomplete space-time dictionary and the corresponding amplitude vector, which depends heavily on clutter distribution and is sensitive to amplitude and phase errors [28, 29]. On the other hand, the sparse recovery STAP is accomplished by adding norm constraint on the weight vector, which is computational intractable and hard to be theoretically analyzed [30, 31].

In this paper, the post-Doppler adaptive processing method, named extended factored approach (EFA or mDT) [34, 35], which is expected to be one of the most efficient and practical STAP algorithms and robust to amplitude and phase errors, are mainly concerned and to be improved. The basic principle of EFA is to transform the full-dimension STAP, which is actually a $KMN$-dimensional ($K$ is the number of pulses, $M$ is the number of transmitting antennas, and $N$ is the number of receiving antennas) adaptive filtering problem, into $K$ separate $PMN$ ($P$ is an integer and $P \geq 2$) dimensional adaptive processing problems. Less training sample requirement and smaller computational cost increase its applicability in practice [36]. However, when insufficient homogeneous training sample support is met, which is a frequent condition especially in the airborne MIMO radar with large-scale antenna array, the clutter suppression ability of EFA will be considerably degraded.

Actually, nowadays the persymmetry property of CCM has received much attention and been used as the a priori knowledge for enhancing CCM estimation. It is initially exploited in communications, [37] extended the application of persymmetry to EFA (Per-EFA), and showed that the required number of training samples was reduced. Per-EFA is verified to be an effective algorithm in training-limited scenarios. However, Per-EFA's computational cost in adaptive processing is increased, and it still requires excessive training samples in the airborne MIMO radar system with large spatial DoFs.

Hence, for the post-Doppler adaptive processing method in the airborne MIMO radar to effectively work, we propose the bi-iterative method for clutter suppression by using persymmetry covariance matrix estimation. Firstly, according to the persymmetry property, CCM is estimated by the original data, the constructed spatial transformed data, the constructed temporal transformed data, and the constructed spatial-temporal transformed data. Secondly, the weight vector in EFA is decomposed into the Kronecker product of two short vectors. Then, the original cost function of EFA is transformed into the cost function with multiple weight vectors. Thirdly, the bi-iterative algorithm [38] is adopted to obtain the desired weight vectors.

### 1.1 Outline

This paper is organized as follows. Fundamentals of the STAP are reviewed in Section 2. Section 3 brings forward the principle of the proposed method, and the computational cost is analyzed in Section 4. In Section 5, the experiments show the performance. Finally, we make a conclusion in Section 6.

### 1.2 Notation

Throughout this paper, matrix and vector are represented by boldface uppercase letter and boldface lowercase letter, respectively. Superscript $^T$, $^*$, and $^H$ separately denote transpose, conjugate, and conjugate transpose of a matrix or a vector. $[\bullet]^{-1}$ means inverse of a matrix. $\otimes$ is the Kronecker product operator. A $c \times c$ identity matrix is denoted as $\mathbf{I}_c$.

## 2 Method and problem setup

Airborne early warning (AEW) radar needs to instantly detect moving targets, which are saturated in the presence of dense ground clutter. It is crucial to suppress the ground clutter. As an effective clutter suppression method in AEW radar, STAP undertakes huge computational cost and excessive training sample requirement, which cannot be fully satisfied in the practical battlefield environment. Moreover, the computational cost and training sample requirement are even huger in MIMO-STAP. Therefore, in this paper, an improving STAP method with tractable computational cost and training sample requirement that applies into the airborne MIMO radar is proposed. The proposed method consists of two parts. The first part is CCM estimation, which is computed according to the original data and the corresponding persymmetry data. The second part is weight vector computation, which is iteratively obtained. We firstly establish the signal model, which will be a foundation for the development and performance analysis of the proposed method.

### 2.1 Signal model

As shown in Fig. 1, the airborne MIMO radar system moves at a constant velocity $v_a$ parallel to the ground. The transmitting array consists of $M$ array elements with interelement space $d_t$ and the receiving array consists of $N$ array elements with interelement space $d_r$. The MIMO radar simultaneously transmits $M$ deterministic

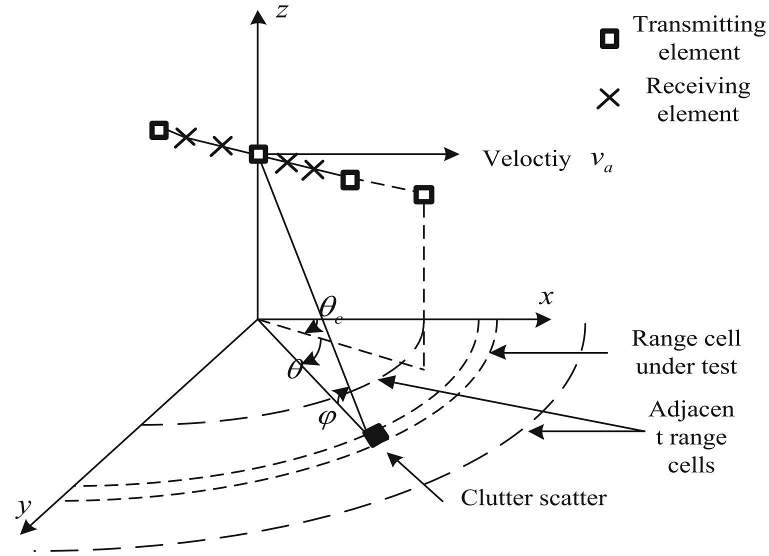


**Fig. 1** Airborne MIMO radar system

waveforms $\mathbf{S} \in \mathbf{C}^{M \times C}$, where $C$ denotes the number of snapshots in each transmitting signal pulse.

The $l$th range cell is uniformly divided into $N_c$ independent clutter patches without consideration of the earth curvature. The location of the $i$thclutter patch is represented by its azimuth angle $\theta_i$ and elevation angle $\phi_l$. Let the crab angle between the antenna array line and the flight velocity be $\theta_c$. Assuming that the MIMO radar system transmits $K$ pulses on the repetition of $T_r$ in one coherent processing interval (CPI), the received clutter matrix on the $l$th range cell at the $k$th pulse is given by [5].

$$\mathbf{Z}(l,k) = \sum_{i=1}^{N_c} \beta_i \exp(j2\pi(k-1)f_{di}) \boldsymbol{a}_r(\theta_i,\phi_l)\boldsymbol{a}_t^T(\theta_i,\phi_l)\mathbf{S}, \quad k = 1,\cdots,K \tag{1}$$

where $f_{di} = 2T_r v_a \cos(\theta_i + \theta_c) \cos\phi_l / \lambda$ is the normalized Doppler frequency, the scatter coefficient $\beta_i$ is clutter echo's random complex amplitude, and $\boldsymbol{a}_t(\theta_i, \phi_l)$ and $\boldsymbol{a}_r(\theta_i, \phi_l)$ are transmitting array steering-vector and receiving array steering-vector, respectively. They are expressed as

$$\begin{aligned} \boldsymbol{a}_t(\theta_i,\phi_l) &= [1,\ \exp(j2\pi f_{si}\alpha), \cdots,\ \exp(j2\pi(M-1)f_{si}\alpha)]^T \\ \boldsymbol{a}_r(\theta_i,\phi_l) &= [1,\ \exp(j2\pi f_{si}), \cdots,\ \exp(j2\pi(N-1)f_{si})]^T, \end{aligned} \tag{2}$$

in which $f_{si} = d_r \cos\theta_i \cos\phi_l / \lambda$ is the normalized spatial frequency, $\lambda$ is the operating wavelength and $\alpha = d_t / d_r$. In order to obtain the sufficient statistics for STAP processing, $\mathbf{S}^H(\mathbf{SS}^H)^{-1/2}$ is employed as the match filter at the receiver. After match filtering and stacking the data in the vector form, the following expression can be obtained

$$\begin{aligned} \mathbf{z}(l,k) &= vec\left[\mathbf{Z}(l,k)\mathbf{S}^H(\mathbf{SS}^H)^{-1/2}\right] \\ &= vec\left[\sum_{i=1}^{N_c} \hat{\beta}_i \exp(j2\pi(k-1)f_{di})\boldsymbol{a}_r(\theta_i,\phi_l)\boldsymbol{a}_t^T(\theta_i,\phi_l)(\mathbf{SS}^H/C)^{1/2}\right] \\ &= \sum_{i=1}^{N_c} \hat{\beta}_i \exp(j2\pi(k-1)f_{di})\hat{\boldsymbol{a}}_t(\theta_i,\phi_l) \otimes \boldsymbol{a}_r(\theta_i,\phi_l), \end{aligned} \tag{3}$$

where $\hat{\beta}_i = \sqrt{C}\beta_i$, $\hat{\boldsymbol{a}}_t(\theta_i,\phi_l) = (\mathbf{S}^*\mathbf{S}^T/C)^{1/2}\boldsymbol{a}_t(\theta_i,\phi_l)$, is the modified transmitting steering-vector. The symbol vec(•) represents the matrix operation that stacks the columns of a matrix under each other to form a new column vector. Now the clutter data received during a CPI is stacked into the vector form as

$$\begin{aligned} \mathbf{z}(l) &= \left[\mathbf{z}^T(l,1), \mathbf{z}^T(l,2), \cdots, \mathbf{z}^T(l,K)\right]^T \\ &= \sum_{i=1}^{N_c} \hat{\beta}_i \boldsymbol{s}_t(f_{di}) \otimes \hat{\boldsymbol{a}}_t(\theta_i,\phi_l) \otimes \boldsymbol{a}_r(\theta_i,\phi_l) \\ &= \sum_{i=1}^{N_c} \hat{\beta}_i \boldsymbol{s}_t(f_{di}) \otimes \boldsymbol{s}_s(\theta_i,\phi_l) = \sum_{i=1}^{N_c} \hat{\beta}_i \mathbf{c}_i, \end{aligned} \tag{4}$$

where $\mathbf{c}_i = \boldsymbol{s}_t(f_{di}) \otimes \boldsymbol{s}_s(\theta_i, \phi_l)$ is the space-time steering-vector with $\boldsymbol{s}_t(f_{di}) = [1, \exp(j2\pi f_{di}), \cdots, \exp(j2\pi(K-1)f_{di})]^T$ and $\boldsymbol{s}_s(\theta_i,\phi_l) = \hat{\boldsymbol{a}}_t(\theta_i,\phi_l) \otimes \boldsymbol{a}_r(\theta_i,\phi_l)$ representing the temporal and spatial steering-vectors, respectively. The received signal contains also the noise, namely,

$$\mathbf{x}(l) = \mathbf{z}(l) + \mathbf{n}, \tag{5}$$

where $\mathbf{n}$ is the white noise vector.

### 2.2 Principle of STAP and EFA

Let the normalized target vector be marked as $\mathbf{s} \in \mathbf{C}^{KMN \times 1}$. The objective of the full-dimension STAP is maintaining the output energy of the target while minimizing that of the clutter. This implies the following cost function

$$\begin{cases} \min E\left[\left|\mathbf{w}^H \mathbf{x}(l)\right|^2\right] \\ s.t. \mathbf{w}^H \mathbf{s} = 1 \end{cases} \tag{6}$$

The Lagrange multiplier methodology can be applied to obtain the optimal weight

$$\mathbf{w} = \mathbf{R}_x^{-1}\mathbf{s} / \left(\mathbf{s}^H \mathbf{R}_x^{-1} \mathbf{s}\right), \tag{7}$$

where $\mathbf{R}_x = E[\mathbf{x}(l)\mathbf{x}^H(l)]$ is the CCM. In general, since the statistics of the clutter range cell under test are never known, CCM is estimated by $L$ secondary training samples in adjacent range cells, namely, $\hat{\mathbf{R}}_x = \frac{1}{L}\sum_{l=1}^{L} \mathbf{x}(l)\mathbf{x}^H(l)$. RMB (Reed, Mallett, and Brennan) rule [36] shows that, in the Gaussian noise environment, if the number of homogeneous training samples exceeds twice the dimension of CCM, the output SCNR (signal-to-clutter-plus-noise ratio) loss will be within 3 dB. The training sample requirement of the full-dimension MIMO-STAP is evidently unpractical. Moreover, as the inverse operation of a $KMN \times KMN$ matrix, the computational complexity is approximate to $O(K^3M^3N^3)$, which is also unbearable. These two major drawbacks prevent the full-dimension MIMO-STAP from being put into effect. Hence, a large number of dimension-reduced MIMO-STAP methods have been developed in the past years. In this paper, the post-Doppler adaptive processing method, namely EFA, is mainly concerned.

EFA performs Doppler filtering on data of each array element and then uses spatial filtering separately within $P$ ($P \geq 2$) Doppler bins [34, 35]. Let $\mathbf{F}_k \in \mathbf{C}^{P \times K}$ be the Doppler filter coefficient vector according to the $k$th ($k = 1, 2, \cdots, K$) Doppler bin, the dimension-reduced transformation matrix can be expressed as

$$\mathbf{T}_k = \mathbf{F}_k \otimes \mathbf{I}_{MN}. \tag{8}$$

The dimension-reduced space-time data and target can be achieved as

$$\begin{aligned} \tilde{\mathbf{x}}_k(l) &= \mathbf{T}_k \mathbf{x}(l) \\ \tilde{\mathbf{s}}_k &= \mathbf{T}_k \mathbf{s} \end{aligned}. \tag{9}$$

The cost function in EFA is

$$\begin{cases} \min E\left[\left|\tilde{\mathbf{w}}_k^H \tilde{\mathbf{x}}_k(l)\right|^2\right] \\ s.t. \tilde{\mathbf{w}}_k^H \tilde{\mathbf{s}}_k = 1 \end{cases} \tag{10}$$

Similarly, the solution to Eq. (10) is obtained by using the Lagrange multiplier methodology and the CCM is estimated by

$$\hat{\mathbf{R}}_{\tilde{x}_k} = \frac{1}{L}\sum_{l=1}^{L} \tilde{\mathbf{x}}_k(l)\tilde{\mathbf{x}}_k^H(l). \tag{11}$$

Evidently, the dimension of CCM is reduced to $PMN$. As a consequence, the required number of training samples and computational cost in adaptive processing are separately reduced to $PMN$ and $O(P^3M^3N^3)$. Although EFA reduce the size of CCM in the adaptive processing, its clutter suppression ability can still be severely degraded due to the insufficient training sample support when antenna array elements are large.

Generally, $P = 3$ is utilized in EFA. Therefore, in the following, the EFA referred in this paper is with three Doppler bins.

## 3 The bi-iterative method using persymmetric covariance matrix estimation

In order to reduce the required number of training samples, the persymmetry is utilized as the a priori knowledge and the CCM is estimated by the following equation [37].

$$\begin{aligned} &\widehat{\mathbf{R}}_{\tilde{x}_k} = \hat{\mathbf{R}}_{\tilde{x}_k} + \mathbf{T}_s \hat{\mathbf{R}}_{\tilde{x}_k}^* \mathbf{T}_s^H + \mathbf{T}_t \hat{\mathbf{R}}_{\tilde{x}_k} \mathbf{T}_t^H + \mathbf{T}_{st} \hat{\mathbf{R}}_{\tilde{x}_k}^* \mathbf{T}_{st}^H / 4 \\ &\mathbf{T}_s = \mathbf{I}_p \otimes \mathbf{J}_s, \mathbf{T}_t = \mathbf{U}_t \otimes \mathbf{I}_{MN}, \mathbf{T}_{st} = \mathbf{U}_{st} \otimes \mathbf{J}_s \end{aligned}, \tag{12}$$

where $\mathbf{U}_t = \mathrm{diag}([\mathrm{e}^{j2\pi f_{k-1}(MN-1)}, \mathrm{e}^{j2\pi f_k(MN-1)}, \mathrm{e}^{j2\pi f_{k+1}(MN-1)}])$, $\mathbf{U}_{st} = \mathrm{diag}([\mathrm{e}^{-j2\pi f_{k-1}(MN-1)}, \mathrm{e}^{-j2\pi f_k(MN-1)}, \mathrm{e}^{-j2\pi f_{k+1}(MN-1)}])$ and $\mathbf{J}_s = \begin{bmatrix} 0 & 0 & 0 & 0 & 1 \\ 0 & 0 & 0 & 1 & 0 \\ \vdots & \vdots & \ddots & \vdots & \vdots \\ 1 & 0 & 0 & 0 & 0 \end{bmatrix} \in \mathbf{C}^{MN \times MN}$

with $f_{k-1}$, $f_k$, $f_{k+1}$, representing the normalized Doppler frequency of three adjacent Doppler bins. After constructing the CCM estimator by Eq. (12), the proposed bi-iterative adaptive method will be introduced. In the following, we will utilize the Kronecker form of weight vector in EFA and further decrease the computational cost and training sample demanding in adaptive processing.

As a matter of fact, the clutter data after dimension-reduced in EFA can be expressed as

$$\begin{aligned} \mathbf{z}(l) &= \mathbf{T}_k \mathbf{z}(l) \\ &= \sum_{i=1}^{N_c} \hat{\beta}_i [\mathbf{F}_k \otimes \mathbf{I}_{MN}][\boldsymbol{s}_t(f_{di}) \otimes \hat{\boldsymbol{a}}_t(\theta_i, \phi_l) \otimes \boldsymbol{a}_r(\theta_i, \phi_l)] \\ &= \sum_{i=1}^{N_c} \hat{\beta}_i \{[\mathbf{F}_k \boldsymbol{s}_t(f_{di})] \otimes [\hat{\boldsymbol{a}}_t(\theta_i, \phi_l)] \otimes [\boldsymbol{a}_r(\theta_i, \phi_l)]\} \\ &= \sum_{i=1}^{N_c} \hat{\beta}_i \left\{\hat{\boldsymbol{a}}_t(\theta_i, \phi_l) \otimes \left[(\mathbf{F}_k \boldsymbol{s}_t(f_{di}))^T \hat{\boldsymbol{a}}_r(\theta_i, \phi_l)\right]\right\} \\ &= \sum_{i=1}^{N_c} \hat{\beta}_i (\mathbf{h} \otimes \mathbf{g}), \end{aligned} \tag{13}$$

where $\mathbf{h} \in \mathbf{C}^{M \times 1} = \hat{\boldsymbol{a}}_t(\theta_i, \phi_l)$ and $\mathbf{g} \in \mathbf{C}^{PN \times 1} = (\mathbf{F}_k \boldsymbol{s}_t)^T \hat{\boldsymbol{a}}_r(\theta_i,$

$\phi_l$). Equation (13) clearly shows that the clutter data after Doppler filtering possesses the structure of the Kronecker products of two vectors. Correspondingly, the adaptive weight vector $\tilde{\mathbf{w}}_k$ can also be supposed to possess the special structure so that $\tilde{\mathbf{w}}_k$ can be decomposed as the Kronecker products of two shorter vectors, namely,

$$\tilde{\mathbf{w}}_k = \mathbf{u} \otimes \mathbf{v}, \tag{14}$$

where $\mathbf{u} \in \mathbf{C}^{a \times 1}$ and $\mathbf{v} \in \mathbf{C}^{b \times 1}$ represent two short weight vectors with $a = M$ and $b = PN$. Substituting Eq. (12) and Eq. (14) into Eq. (10) yields the following cost function

$$\begin{cases} \min(\mathbf{u} \otimes \mathbf{v})^H \widehat{\mathbf{R}}_{\tilde{x}_k} (\mathbf{u} \otimes \mathbf{v}) \\ s.t. (\mathbf{u} \otimes \mathbf{v})^H \tilde{\mathbf{s}}_k = 1 \end{cases} \tag{15}$$

Using the Lagrange multiplier methodology, cost function (15) can be transformed into the following unconstrained one

$$J(\mathbf{u}, \mathbf{v}) = (\mathbf{u} \otimes \mathbf{v})^H \widehat{\mathbf{R}}_{\tilde{x}_k} (\mathbf{u} \otimes \mathbf{v}) + \mu \left(1 - (\mathbf{u} \otimes \mathbf{v})^H \tilde{\mathbf{s}}_k \right), \tag{16}$$

where $\mu$ is the Lagrange multiplier. Generally, the solution to Eq. (16) is not easy to be analytically expressed. But fortunately, the cyclic minimizer [38] can be conveniently applied to numerically solve this cost function.

To obtain the numerical solution to Eq. (16), $\mathbf{u}$ is initialized with $\mathbf{u}(0)$. Then, Eq. (16) becomes an unconstrained cost function with respect to $\mathbf{v}$ and $\mu$ after substituting $\mathbf{u}(0)$ into it. Letting the gradient of $J(\mathbf{u}(0), \mathbf{v})$ with respect to $\mathbf{v}$ and $\mu$ be zero yields an iterative value

$$\mathbf{v}(1) = \mathbf{R}_v^{-1} \mathbf{s}_v / \left( \mathbf{s}_v^H \mathbf{R}_v^{-1} \mathbf{s}_v \right), \tag{17}$$

where

$$\mathbf{R}_v = (\mathbf{u}(0) \otimes \mathbf{I}_b)^H \widehat{\mathbf{R}}_{\tilde{x}_k} (\mathbf{u}(0) \otimes \mathbf{I}_b), \mathbf{s}_v = (\mathbf{u}(0) \otimes \mathbf{I}_b)^H \tilde{\mathbf{s}}_k. \tag{18}$$

Again, with fixing $\mathbf{v}(1)$, let the gradient of $J(\mathbf{u}, \mathbf{v}(1))$ with respect to $\mathbf{u}$ and $\mu$ be zero, the iterative value of $\mathbf{u}(1)$ can be achieved by

$$\mathbf{u}(1) = \mathbf{R}_u^{-1} \mathbf{s}_u / \left( \mathbf{s}_u^H \mathbf{R}_u^{-1} \mathbf{s}_u \right), \tag{19}$$

where

$$\mathbf{R}_u = (\mathbf{I}_a \otimes \mathbf{v}(1))^H \widehat{\mathbf{R}}_{\tilde{x}_k} (\mathbf{I}_a \otimes \mathbf{v}(1)), \mathbf{s}_u = (\mathbf{I}_a \otimes \mathbf{v}(1))^H \tilde{\mathbf{s}}_k. \tag{20}$$

By repeating the aforementioned iterative procedure, $\mathbf{v}(t)$ and $\mathbf{v}(2)$, $\mathbf{u}(3)$ and $\mathbf{v}(3)$, …, can be obtained in turn. The iterative procedure will be stopped if the termination condition $\|\mathbf{v}(t) - \mathbf{v}(t-1)\| / \|\mathbf{v}(t)\| < \delta$ is satisfied at the $t$th iteration, where $\delta$ is the threshold and $\|\bullet\|$ is the Euclidean norm of a vector. The bi-iterative algorithm is summarized in Table 1.

Finally, $\mathbf{u}(t)$ and $\mathbf{v}(t)$ are substituted into (14) and $\tilde{\mathbf{w}}_k$ is achieved by the Kronecker product of two short vectors

$$\tilde{\mathbf{w}}_k = \mathbf{u}(t) \otimes \mathbf{v}(t). \tag{21}$$

The sizes of $\mathbf{R}_u$ and $\mathbf{R}_v$ produced in the iterative procedure are $a \times a$ and $b \times b$ respectively. After weight decomposition, both the required number of training samples and computational cost in the spatial adaptive processing are reduced. Hereafter, for convenience, EFA that uses Eq. (12) as CCM estimation is marked as MIMOPer-EFA, EFA based on the bi-iterative algorithm using Eq. (11) as CCM estimation is marked as MIMOBi-EFA, and EFA based on the bi-iterative algorithm using Eq. (12) as CCM estimation is marked as MIMOBiPer-EFA.

## 4 Convergence and computational cost analysis

In this section, the asymptotic convergence of the bi-iterative algorithm is analyzed and verified. First of all, two definitions and one theorem will be introduced [39]:

Definition 1 (Lyapunov function): let the set $\mathbb{R}$ be defined by $\mathbb{R} = \{\mathbf{h} | \mathbf{h} \in \mathbf{C}^{\tilde{m} \times \tilde{n}}\}$. A function $f(\mathbf{h})$ defined in $\mathbb{R}$ is called a Lyapunov function associated with a discrete sequence $\mathbf{h}(t)$, if (1) $f(\mathbf{h})$ is continuous; (2) the set $\mathbf{g}_c = \{\mathbf{h} | f(\mathbf{h}) < c\}$ is bounded for any finite positive constant $c$; (3) $f(\mathbf{h}(t)) \le f(\mathbf{h}(t-1))$ for a discrete time $t$.

Definition 2 (invariance set): if the discrete sequence $\mathbf{h}(t) \in \mathbb{R}$, then the set $\mathbb{R}_{\text{Inva}} = \{\mathbf{h}(t) | f(\mathbf{h}(t)) - f(\mathbf{h}(t-1)) = 0\}$ is called the invariance set of $\mathbf{h}(t)$.

Theorem (LaSalle invariance theorem): if function $f(\mathbf{h}(t))$ is the Lyapunov function with respect to the discrete sequence $\mathbf{h}(t) \in \mathbb{R}$, then $\mathbf{h}(t)$converges to the invariance set $\mathbb{R}_{\text{Inva}}$.

Next, we will show that $J(\mathbf{u}, \mathbf{v})$ satisfy the three conditions defined in Lyapunov function by transforming $J(\mathbf{u}, \mathbf{v})$ to $J(\mathbf{h})$ with $\mathbf{h} = \mathbf{u} \otimes \mathbf{v}$. Firstly, the cost function $J(\mathbf{h})$ is continuous for its differentiability. Secondly, $J(\mathbf{h}(t-1)) \ge J(\mathbf{h}(t))$ since

$$\begin{aligned} J(\mathbf{h}(t-1)) &= J(\boldsymbol{u}(t-1), \boldsymbol{v}(t-1)) \ge J(\boldsymbol{u}(t-1), \boldsymbol{v}(t)) \\ &= \min_{v} J(\boldsymbol{u}(t-1), \boldsymbol{v}) \ge J(\boldsymbol{u}(t), \boldsymbol{v}(t)) \\ &= \min_{u} J(\boldsymbol{u}, \boldsymbol{v}(t)) = J(\mathbf{h}(t)). \end{aligned} \tag{22}$$

Thirdly, let $\|\mathbf{v}\| = 1$; the relation $J(\mathbf{u}(t), \mathbf{v}(t)) = \mathbf{u}^H \mathbf{R}_u \mathbf{u} \ge \lambda_{\min} \|\mathbf{u}\|^2$ can be acquired and the set $\{\mathbf{u}(t) | \lambda_{\min} \|\mathbf{u}(t)\|^2 \le J(\mathbf{u}(t), \mathbf{v}(t)) \le c\}$ is bounded for any constant $0 < c < \infty$, where $\lambda_{\min}$ is the smallest eigenvalue of $\mathbf{R}_u$. Therefore, the set $\{\mathbf{h}(t) | J(\mathbf{h}(t)) \le c\}$ bounded for any constant $0 < c < \infty$ and any iteration number $tt$ is inferred. The three points just mentioned above satisfy the definition of Lyapunov function. As a consequence, according to LaSalle

**Table 1** Bi-iterative algorithm

**Input**: $\widehat{\mathbf{R}}_{\tilde{x}_k}$, $\tilde{\mathbf{s}}_k$, error tolerance $\delta$.

**Initialize**: $\mathbf{u}(0)$, $t=1$.

**For** t=1,2,3... **do**

**Update** $\mathbf{u}$ and $\mathbf{v}$

$\mathbf{v}(t)=\mathbf{R}_v^{-1}\mathbf{s}_v/(\mathbf{s}_v^H\mathbf{R}_v^{-1}\mathbf{s}_v)$,

where $\mathbf{R}_v=(\mathbf{u}(t-1)\otimes\mathbf{I}_b)^H\widehat{\mathbf{R}}_{\tilde{x}_k}(\mathbf{u}(t-1)\otimes\mathbf{I}_b)$, $\mathbf{s}_v=(\mathbf{u}(t-1)\otimes\mathbf{I}_b)^H\tilde{\mathbf{s}}_k$.

$\mathbf{u}(t)=\mathbf{R}_u^{-1}\mathbf{s}_u/(\mathbf{s}_u^H\mathbf{R}_u^{-1}\mathbf{s}_u)$,

where $\mathbf{R}_u=(\mathbf{I}_a\otimes\mathbf{v}(t))^H\widehat{\mathbf{R}}_{\tilde{x}_k}(\mathbf{I}_a\otimes\mathbf{v}(t))$, $\mathbf{s}_u=(\mathbf{I}_a\otimes\mathbf{v}(t))^H\tilde{\mathbf{s}}_k$.

$t=t+1$.

**Stop if** $\|\mathbf{v}(t)-\mathbf{v}(t-1)\|/\|\mathbf{v}(t)\|<\delta$ is satisfied.

**End for**

invariance principle [39], $J(\mathbf{h})$ is the Lyapunov function. By using the LaSalle invariance theorem, the conclusion that the cost function $J(\mathbf{h})$ is asymptotically convergent can be obtained [40].

After the convergence analysis, the computational costs of MIMOBiPer-EFA, MIMOBi-EFA, MIMOPer-EFA, and EFA will be analyzed. Since the computational costs of the Doppler filtering are nearly the same in each method, we mainly consider the computational costs of CCM estimation and weight vector calculation in spatial adaptive processing. The multiplication and division number (MDN) is used as an index of the computational cost. First of all, the computational cost of MIMOBiPer-EFA is analyzed in detail. It should be noted that the MDN of CCM estimation by Eq. (12), Eq. (18), and Eq. (20) is $L_1[3(3MN)^2+3aMN+3bMN+a^2+b^2]$. The MDN of weight vectors computed by Eq. (17) and Eq. (19) is $\frac{2}{3}[a^3+b^3]+2a^2+a+2b^2+b$. As shown in Fig. 9, the bi-iterative algorithm can reach the convergence value within 10 steps. Therefore, the total MDN of MIMOBiPer-EFA is

$$L_1\left[3(3MN)^2+3aMN+3bMN+a^2+b^2\right]+\frac{20}{3}\left[a^3+b^3\right]+10\left[2a^2+a+2b^2+b\right]. \tag{23}$$

Similarly, the MDNs of EFA, MIMOPer-EFA, and MIMOBi-EFA are

$$\begin{aligned}&L_4(3MN)^2+\frac{2}{3}(3MN)^3+2(3MN)^2+3MN\\&L_3\left[3(3MN)^2+(3MN)^2\right]+\frac{2}{3}(3MN)^3+2(3MN)^2+3MN\\&L_2\left[3aMN+3bMN+a^2+b^2\right]+\frac{20}{3}\left[a^3+b^3\right]+10\left[2a^2+a+2b^2+b\right],\end{aligned} \tag{24}$$

respectively, where $L_1$, $L_2$, $L_3$ and $L_4$ are the required number of training samples in each method. As the comparison, the MDNs of classic sample matrix inversion (SMI) and principal component (PC) are calculated as follows:

$$\begin{aligned}&L_6(KMN)^2+\frac{2}{3}(KMN)^3+2(KMN)^2+KMN\\&L_5(KMN)^2+\frac{2}{3}(KMN)^3+r_c(KMN)^2\end{aligned}, \tag{25}$$

where $L_5$ and $L_6$ are the required number of training samples in PC and SMI, $r_c$ is the clutter rank.

## 5 Experimental results and discussion

### 5.1 Simulation results

In the simulations, the quadrature phase shift keyed (QPSK) signal with snapshots $C=256$ is transmitted by the airborne MIMO radar. Both the numbers of uniform linear transmitting array elements and receiving array elements are 8. The other necessary parameters for the simulation are listed in Table 2.

Intuitively, $\tilde{\mathbf{w}}_k$ can be decomposed as the Kronecker product of $\mathbf{u}$ and $\mathbf{v}$ with different dimensions. Therefore, many decomposition results, such as $a=2$ and $b=96$, $a=3$ and $b=64$, and $a=6$ and $b=32$,... satisfy $a\times b=3MN$. Actually, the more $a$ is close to $b$, the less computational cost and the number of training samples will be required in adaptive processing. We will demonstrate

**Table 2** Parameters of the simulation

| Parameter | Value |
|---|---|
| Transmitting array element spacing | $d_t=0.2$ m |
| Receiving array element spacing | $d_r=0.1$ m |
| Wavelength | $\lambda=0.2$ m |
| Pulse repetition frequency (PRF) | PRF = 2000 Hz |
| Number of pulses in a CPI | $K=16$ |
| Platform velocity | $v_a=100$ m/s |
| Platform height | $h=9$ km |

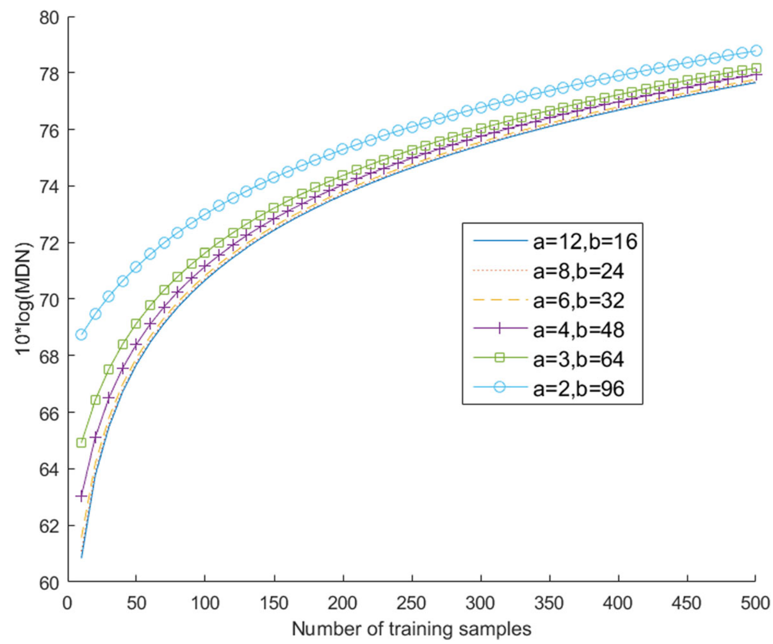


**Fig. 2** Computational costs for different *a* and *b*

the fact by the following computational cost comparison and training sample convergence rate comparison simulations. In Fig. 2, the computational costs for different *a* and *b* are compared. It can be shown that MIMOBiPer-EFA can achieve the minimum computational cost when $a = 12$ and $b = 16$. Similarly, as shown in Fig. 3, MIMOBiPer-EFA possesses the fastest training sample convergence rate when $a = 12$ and $b = 16$. However, the computational costs and training sample convergence rates of MIMOBiPer-EFA with $a = 12$ and $b = 16$ and MIMOBiPer-EFA with $a = 8$ and $b = 24$ are nearly the same. In addition, the steady-state value of MIMOBiPer-EFA with $a = 8$ and $b = 24$is slightly higher than that of MIMOBiPer-EFA with $a = 16$ and $b = 12$. Therefore, in view of the SCNR performance, training sample requirement and in accordance with the Kronecker form in Eq. (14), $a = 8$ and $b = 24$ is chosen in our simulations.

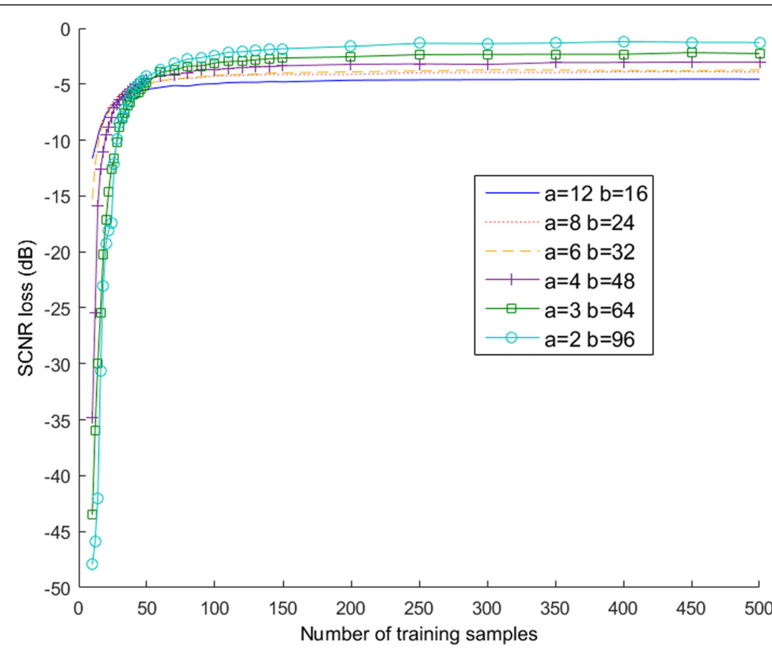


**Fig. 3** Training sample convergence rates for different *a* and *b*

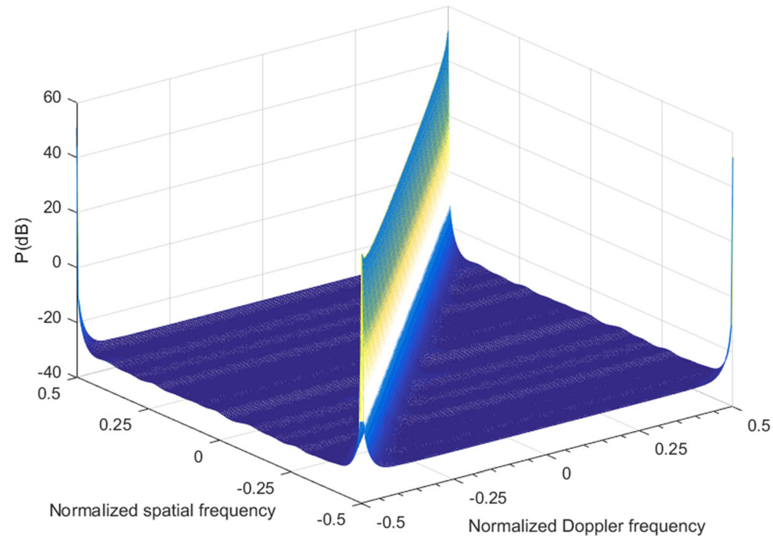


**Fig. 4** MVDR spectrum of clutter

Figure 4 shows the minimum variance distortionless response (MVDR) power spectrum of the clutter. It is clearly seen that the clutter distributes along the diagonal on the plane. Various STAP methods can be performed to sufficiently suppress the clutter that may be evidently stronger than targets. One important metric to measure the clutter suppression ability of STAP methods is the SCNR loss, which is defined as the loss between the implemented processor and the optimal one [5]. According to the parameters given above, the weight vector in EFA is decomposed into the Kronecker product of two short vectors with $\mathbf{u} \in \mathbf{C}^{N \times 1}$ and $\mathbf{v} \in \mathbf{C}^{3M \times 1}$. A fast-converging STAP method named fast maximum likelihood (FML) estimator proposed by Gerlach and Picciolo is adopted here as the comparison [41]. Figure 5 shows the SCNR loss curves of MIMOBiPer-EFA, MIMOBi-EFA, MIMOPer-EFA, EFA, and FML with 500 homogeneous training samples support. Under this condition, FML can achieve the best SCNR performance. The SCNR performance of MIMOBiPer-EFA is slightly worse than those of MIMOBi-EFA, MIMOPer-EFA, and EFA. Figures 6 and 7 show the SCNR loss curves with small training samples support. Twenty training samples are adopted.[1] In addition, $\theta_c = 0$ that represents the sidelooking scenario and $\theta_c = \pi/6$ that represents the non-sidelooking scenario are considered. It is demonstrated that when limited training samples are met, which is a frequent condition especially in the airborne MIMO radar, MIMOBiPer-EFA will evidently outperform MIMOBi-EFA, MIMOPer-EFA, EFA, and FML both in main clutter region and sidelobe clutter region. In addition, MIMOBi-EFA, MIMOPer-EFA, EFA, and

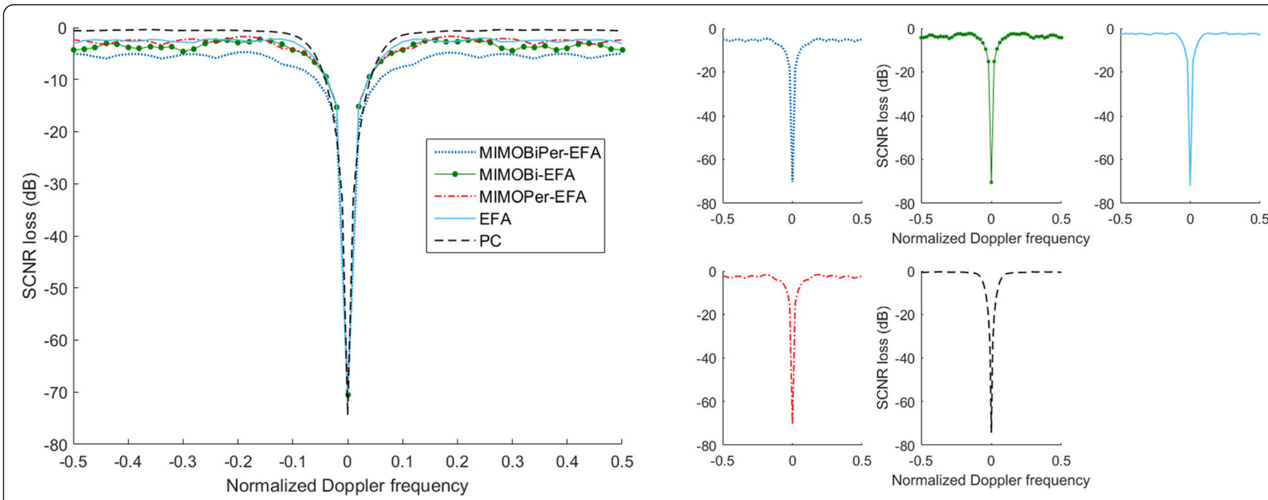


**Fig. 5** SCNR loss curves with large training samples support ($L = 500$)

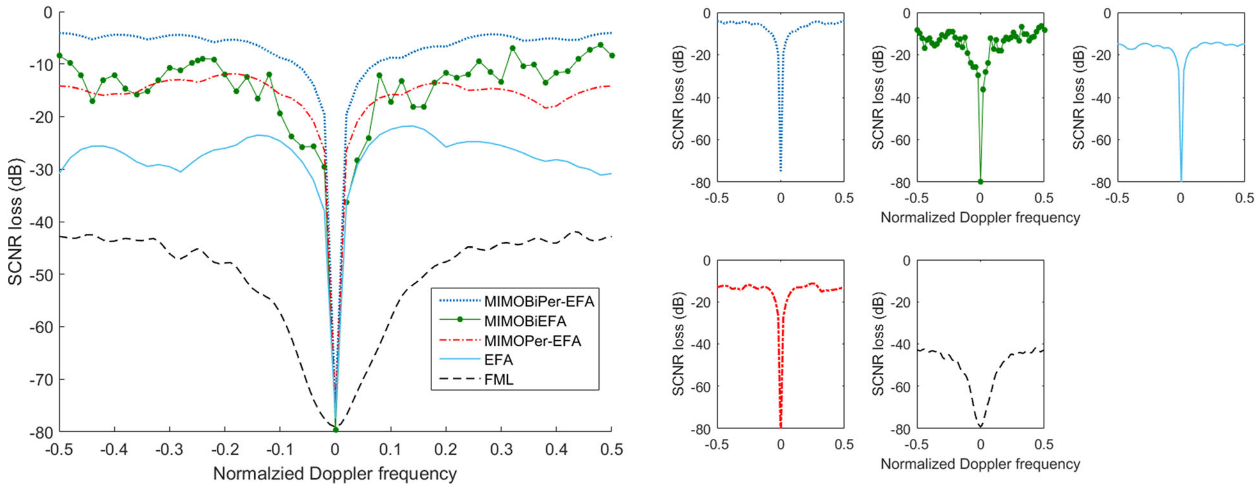


**Fig. 6** SCNR loss curves with small training samples support under sidelooking scenario ($L = 20$)

FML bear great performance losses when the number of training samples becomes small. However, the SCNR loss performance of MIMOBiPer-EFA keeps nearly the same as shown in Fig. 5.

The SCNR loss versus the number of training samples describes the training sample convergence rate of a STAP method. Figure 8 compares the training sample convergence rates of each method at the normalized Doppler frequency 0.3 and the normalized spatial frequency 0, where 100 independent Monte Carlo runs are conducted to achieve each point. The initial training sample numbers of MIMOBiPer-EFA, MIMOBi-EFA, MIMOPer-EFA, EFA, and FML are 10, 30, 50, 200, and 40, separately. Obviously, MIMOBiPer-EFA enjoys faster convergence rate than its counterparts. Though FML also converges fast and can achieve superior steady-state SCNR performance to MIMOBiPer-EFA, it behaves poorer performance than MIMOBi-EFA when the number of training samples is smaller than 50. Figures 6 and 7 also verify the fact. Moreover, as exhibited in Fig. 9, the bi-iterative algorithm can reach the convergence value in 10 iterations, which demonstrates its fast iterative convergence rate. However, one point should be noted here that due to using the optimum processing in spatial domain, better SCNR loss performance can be obtained by MIMOPer-EFA and EFA when adequate number of training samples is available.

According to Eq. (23), Eq. (24), and Eq. (25), the computational cost comparison is shown in Fig. 10. For simplicity, the number of receiving antenna elements is set to be equal with the number of transmitting antenna elements. $L_1 = 30$, $L_2 = 80$, $L_3 = 150$ $L_4 = 300$, $L_5 = 2r_c$, and $L_6 = 2KMN$ are adopted here since each method can

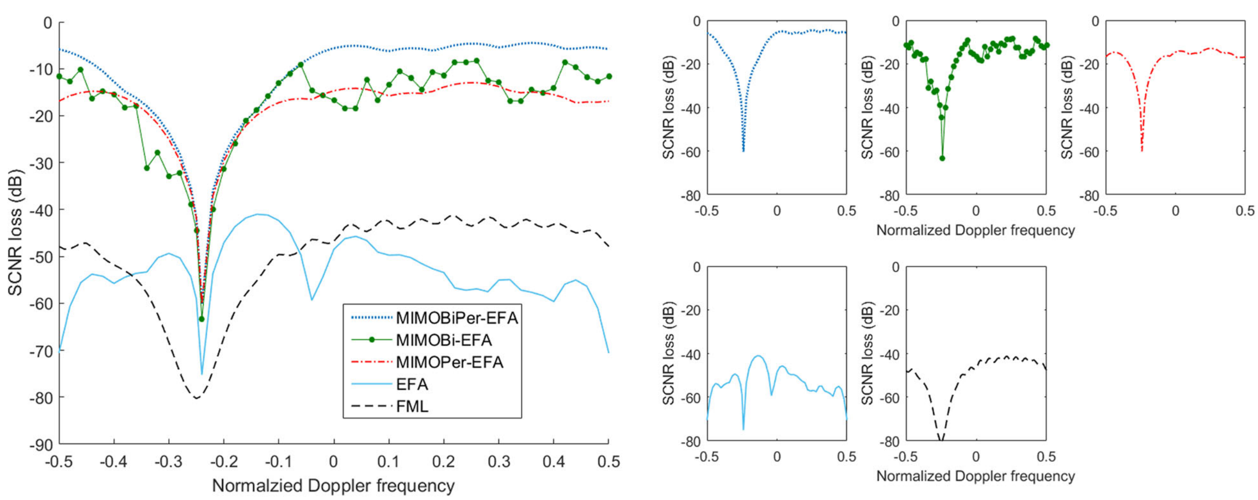


**Fig. 7** SCNR loss curves with small training samples support under non-sidelooking scenario ($L = 20$)

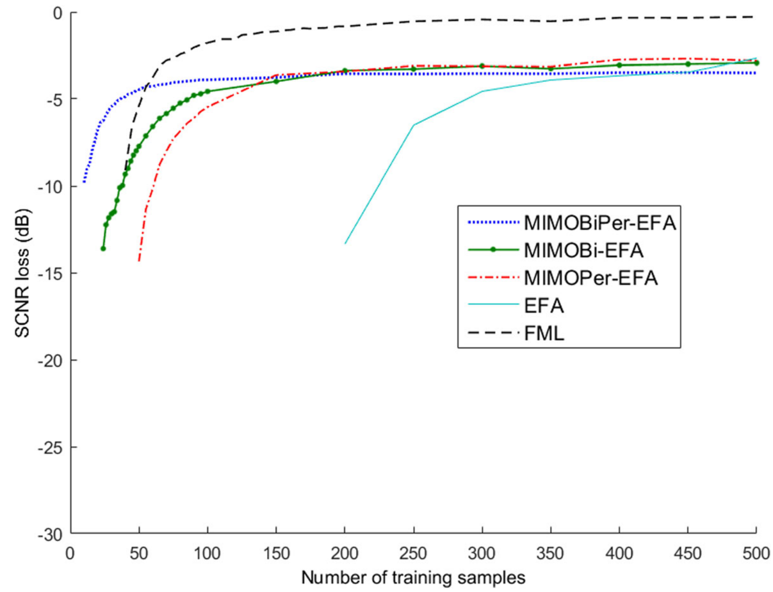


**Fig. 8** The convergence rate comparison

acquire nearly the same SCNR loss with the chosen number of training samples. The computational cost of SMI and PC are obviously several orders of magnitude greater than other methods. In addition, the computational cost of FML is almost the same as that of PC. Compared with MIMOBi-EFA, MIMOBiPer-EFA can achieve the smaller training sample requirement but at the higher computational cost for the extra computational cost increased in CCM estimation. However, MIMOBiPer-EFA still possesses smaller computational cost than those of MIMOPer-EFA and EFA.

### 5.2 MCARM data

In order to verify a good many achievements in the theory of STAP, MCARM program was established by Rome Laboratory and Northrop Grumman Corporation [42]. The MCARM data used in the experiment comes from acquisition 575 on flight 5 (rl050575). Though the MCARM data are not adopted from the airborne MIMO radar system, it is still worth applying to verify the proposed method. In addition, BiPer-EFA, Bi-EFA, and Per-EFA are the suitable names here for representing the corresponding method. The operating parameters used

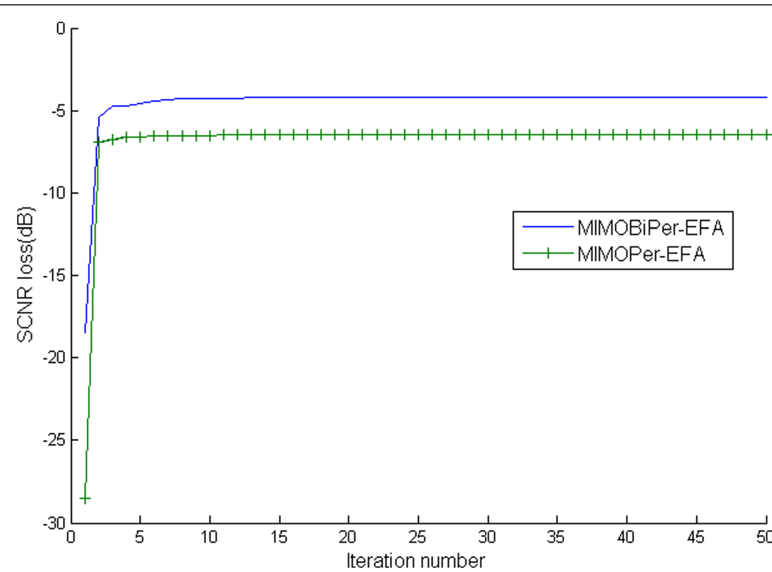


**Fig. 9** The iterative convergence rate

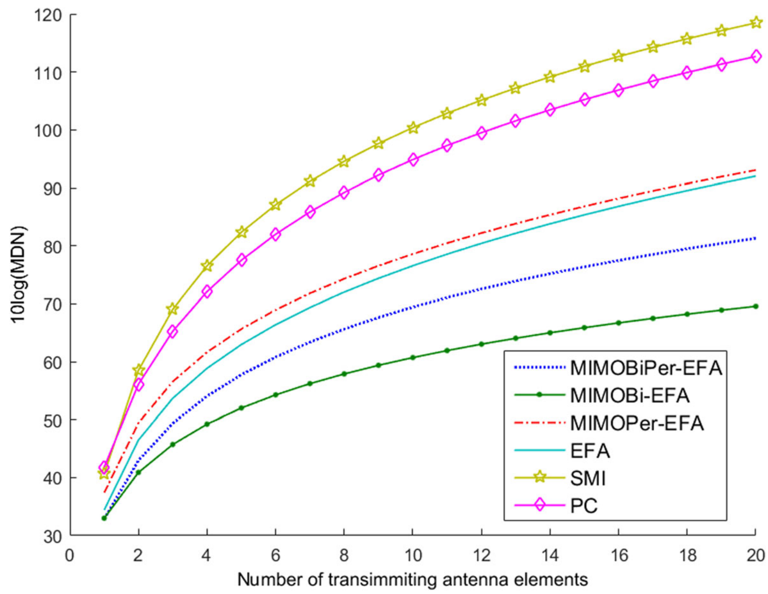


**Fig. 10** Computational cost comparison

to obtain the data are as follows: the platform velocity $v = 100.2$ m/s, the crab angle $\theta_c = 7.28^{\circ}$, the array element spacing $d = 0.1092$ m, the radar operating wavelength $\lambda = 0.2419$ m, the pulse repetition frequency $f_r = 1984$ Hz. 250–500 range bins are selected to verify the proposed algorithm. The first 10 azimuth channels and the first 32 pulses are exploited here. Accordingly, the length of weight vector in EFA is 30, and it can be decomposed into the Kronecker product of two short vectors with $\mathbf{u} \in \mathbf{C}^{5\times 1}$ and $\mathbf{v} \in \mathbf{C}^{6\times 1}$. Two SNR = − 40 dB moving targets with azimuth angles 90° and Doppler frequency $f_d = -0.157 f_r$ are separately injected near the clutter main beam at the range bins 350 and 370. Figure 11 shows the normalized output power (NOP) of each range bin

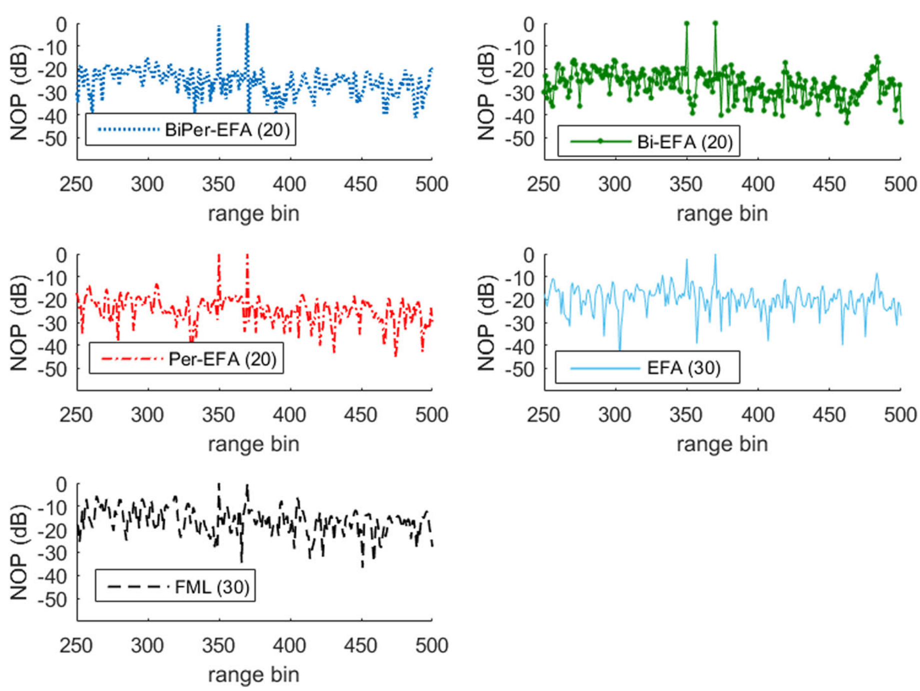


**Fig. 11** Curves of NOP against range bins of different methods

by making use of the BiPer-EFA, Bi-EFA, Per-EFA, EFA, and FML, in which the number of training samples for CCM estimation are marked in the parentheses. It is clearly demonstrated that all these methods can identify the two weak targets from the residual clutter. The average NOP below the target of the BiPer-EFA, Bi-EFA, Per-EFA, EFA, and FML are about 26.85 dB, 25.87 dB, 24.93 dB, 20.06 dB, and 17.26 dB, respectively. The results infer that the proposed algorithms can achieve relatively good performance at the improvement of output SCNR and the corresponding detection probability.

## 6 Discussion

Based on the obtained results, the following conclusions can be obtained:

(1) The proposed MIMOBiPer-EFA is an effective clutter suppression method when the number of training samples is small. The computational cost and training sample demanding of MIMOBiPer-EFA are tractable. MIMOBiPer-EFA is even more advantageous when the large-scale antenna array is applied in the airborne MIMO radar system.
(2) MIMOBiPer-EFA enjoys faster training sample convergence rate than MIMOBi-EFA while it possesses larger computational cost than MIMOBi-EFA for the extra persymmetry CCM estimation. Therefore, MIMOBiPer-EFA will be the desired method if the required number of training samples is the dominant metric while MIMOBi-EFA will be the desired one if the computational cost is the dominant metric.
(3) When the number of training sample is large enough, the SCNR loss performances of EFA, MIMOPer-EFA, and FML are superior to that of MIMOBiPer-EFA. The probable reason for this result is that when adequate number of training samples is available, MIMOPer-EFA and EFA can achieve the optimal SCNR values while MIMOBiPer-EFA can only achieve an inferior SCNR value for the limitation of the special structure of weight vector.

## 7 Conclusions

A method that decreases the training sample requirement and computational cost in the airborne MIMO radar for clutter suppression has been proposed. It estimates CCM by the persymmetry property. Then, the weight vector is constructed as the Kronecker product of two short weight vectors. The bi-iterative method is applied to find the desired result. Simulation results show that the proposed method is advantageous in convergence rate and training sample requirement. The proposed method has greater clutter suppression ability compared with the previously proposed post-Doppler adaptive processing methods especially in the airborne MIMO radar with limited homogeneous training sample support.

## 8 Endnotes

[1]Notice that under this condition, if the estimated CCM is singular, the pseudo inverse of the estimated CCM instead of its inverse is utilized

### Abbreviations

CCM: Clutter covariance matrix; CPI: Coherent processing interval; DoFs: Degrees of freedom; EFA: Extended factored approach; FML: Fast maximum likelihood; MDN: Multiplication and division number; MIMO: Multiple-input multiple-output; Per-EFA: Persymmetry EFA; PRF: Pulse repetition frequency; QPSK: Quadrature phase shift keyed; RMB: Reed, Mallett, and Brennan; SCNR: Signal-to-clutter-plus-noise ratio; SIMO: Single-input multiple-output; STAP: Space-time adaptive processing

### Acknowledgements

This work was sponsored in part by National Natural Science Foundation of China under Grants 61801384, 61503300 and 41601353; the Scientific Research Plan of Education Department of Shaanxi Province under Grant 17JK0789.

### Funding

National Natural Science Foundation of China under Grants 61801384, 61503300 and 41601353; the Scientific Research Plan of Education Department of Shaanxi Province under Grant 17JK0789.

### Availability of data and materials

Since our laboratory is a military secrecy department, parts of data and material cannot be available.

### Authors' contributions

YZ and LW conceived the algorithm and wrote the paper. YL designed the experiments and BJ conducted the simulations. XC made the contribution to the computational analysis and helped revise the paper. Finally, DF checked the whole paper. All authors read and approved the final manuscript.

### Competing interests

The authors declare that they have no competing interests.

## Publisher's Note



Received: 21 January 2018 Accepted: 28 January 2019
Published online: 22 February 2019

### References

1. D.W. Bliss, K.W. Forsythe, in *Proc. 37th IEEE Asilomar Conf. Signal, Systems, Computers, 1*. Multiple-input multiple-output (MIMO) radar and imaging: Degrees of freedom and resolution (2003), pp. 54–49
2. E. Fisher, A. Haimovich, R. Blum, et al., in *Proc. 2004 IEEE Radar Conf*. MIMO radar: An idea whose time has come (2004), pp. 71–78
3. H. Yang, J. Chun, An improved algebraic solution for moving target localization in noncoherent MIMO radar systems. IEEE Trans. Signal Process. **64**(1), 258–270 (2016)
4. N. Shahbazi, A. Abbasfar, M. Jabbarian-Jahromi, Efficient two-dimensional compressive sensing in MIMO radar. EURASIP J. Adv. Signal Process. **2017**(1), 23 (2017)
5. C.Y. Chen, P.P. Vaidyanathan, MIMO radar space-time adaptive processing using prolate spheroidal wave functions. IEEE Trans. Signal Process. **56**(2), 623–635 (2007)
6. C. Xiang, D.Z. Feng, H. Lv, et al., Three-dimensional reduced-dimension transformation for MIMO radar space–time adaptive processing. Signal Process. **91**(8), 2121–2126 (2011)

7. X. Yu, G. Cui, M. Piezzo, et al., Robust constrained waveform design for MIMO radar with uncertain steering vectors. EURASIP J. Adv. Signal Process. **2017**(1), 2 (2017)
8. F. Brigui, M. Boizard, G. Ginolhac, et al., New low-rank filters for MIMO-STAP based on an orthogonal tensorial decomposition. IEEE Trans. Aerosp. Electron. Syst. **54**(3), 1208–1220 (2017)
9. Y. Bar-Shalom, P.K. Willett, X. Tian, in *CT : YBS Publishing*. Tracking and data fusion: A handbook of algorithms. Storrs (2011)
10. R. Mahler, *Statistical multisource-multitarget information fusion* (Artech House, Norwood, 2007)
11. F. Meyer, T. Kropfreiter, J.L. Williams, et al., Message passing algorithms for scalable multitarget tracking. Proc. IEEE **106**(2), 221–259 (2018)
12. J.R. Guerci, *Space-time adaptive processing for radar* (Artech House, Norwood, 2003)
13. H. Wang, L. Cai, On adaptive spatial-temporal processing for airborne surveillance radar systems. IEEE Trans. Aerosp. Electron. Syst. **30**(3), 660–670 (1994)
14. M. Rangaswamy, Statistical analysis of the nonhomogeneity detector for non-Gaussian interference backgrounds. IEEE Trans. Signal Process. **53**(6), 2101–2111 (2005)
15. W.L. Melvin, Space-time adaptive radar performance in heterogeneous clutter. IEEE Trans. Aerosp. Electron. Syst. **36**(2), 621–633 (2000)
16. W. Zhang, Z. He, J. Li, et al., A method for finding best channels in beam-space post-Doppler reduced-dimension STAP. IEEE Trans. Aerosp. Electron. Syst. **50**(1), 254–264 (2014)
17. Y. Zhou, D. Feng, G. Zhu, et al., The post-Doppler adaptive processing method based on the spatial domain reconstruction. Signal Process. **111**(C), 89–93 (2015)
18. R. Li, J. Li, W. Zhang, et al., Reduced-dimension space-time adaptive processing based on angle-Doppler correlation coefficient. EURASIP. J. Adv. Signal Process. **2016**(1), 97 (2016)
19. A.M. Haimovich, Y. Bar-Ness, An eigenanalysis interference canceler. IEEE Trans. Signal Process. **39**(1), 76–84 (1991)
20. J.S. Goldstein, I.S. Reed, Subspace selection for partially adaptive sensor array processing. IEEE Trans. Aerosp. Electron. Syst. **33**(2), 539–544 (2002)
21. X. Mestre, M.A. Lagunas, Finite sample size effect on minimum variance beamformers: Optimum diagonal loading factor for large arrays. IEEE Trans. Signal Process. **54**(1), 69–82 (2005)
22. M. Boizard, G. Ginolhac, .F Pascal, et al, Low-rank filter and detector for multidimensional data based on an alternative unfolding HOSVD: Application to polarimetric STAP. EURASIP J. Adv. Signal Process. 2014(1):119 (2014)
23. S. Haykin, Cognitive radar: A way of future. IEEE Signal Process. Mag. **23**(1), 30–40 (2006)
24. R. Adve, T. Hale, M. Wicks, Knowledge based adaptive processing for ground moving target indication. Digit. Signal Process. **17**(2), 495–514 (2007)
25. A. Aubry, V. Carotenuto, A.D. Maio, et al., Exploiting multiple a priori spectral models for adaptive radar detection. IET Radar Sonar & Navigation **8**(7), 695–707 (2014)
26. Y. Wang, Z. He, Thinned knowledge-aided STAP by exploiting structural covariance matrix. IET Radar Sonar & Navigation **11**(8), 1266–1275 (2017)
27. G. Sun, Z. He, J. Tong, et al., Knowledge-aided covariance matrix estimation via Kronecker product expansions for airborne STAP. IEEE Geosci. Remote Sens. Lett. **15**(4), 527–531 (2018)
28. K. Sun, H. Meng, F.D. Lapierre, et al., Registration-based compensation using sparse representation in conformal-array STAP. Signal Process. **91**(10), 2268–2276 (2017)
29. Z. Yang, X. Li, H. Wang, et al., Knowledge-aided STAP with sparse-recovery by exploiting spatio-temporal sparsity. IET Signal Process. **10**(2), 150–161 (2016)
30. X. Yang, Y. Sun, T. Zeng, et al., Fast STAP method based on PAST with sparse constraint for airborne phased array radar. IEEE Trans. Signal Process. **64**(17), 4550–4561 (2016)
31. S. Qiu, X. Ma, W. Sheng, et al., Robust adaptive monopulse algorithm based on main lobe constraints and subspace tracking. EURASIP J. Adv. Signal Process. **2017**(1), 14 (2017)
32. A. Aubry, A.D. Maio, L. Pallotta, et al., Median matrices and their application to radar training data selection. IET Radar Sonar Navigation **8**(4), 265–274 (2014)
33. A. Aubry, A.D. Maio, L. Pallotta, A geometric approach to covariance matrix estimation and its applications to radar problems. IEEE Trans. Signal Process. **66**(4), 907–922 (2018)
34. R.C. DiPietro, *Extended factored space-time processing for airborne radar systems* (Proc. 26th Asilomar Conf. Signal, Syst. Comput, Pacific Grove, 1992), pp. 425–430
35. Z. Bao, G.S. Liao, R.B. Wu, et al., Adaptive spatial-temporal processing for airborne radars. Chin. J. Electron. **2**(1), 1–7 (1993)
36. I.S. Reed, J.D. Mallett, L.E. Brennan, Rapid convergence rate in adaptive arrays. IEEE Trans. Aerosp. Electron. Syst. **10**(6), 853–863 (1974)
37. Y. Tong, T. Wang, J. Wu, Improving EFA-STAP performance using persymmetric covariance matrix estimation. IEEE Trans. Aerosp. Electron. Syst. **51**(2), 924–936 (2015)
38. P. Stoica, Y. Selen, Cyclic minimizers, majorization techniques, and the expectation-maximization algorithm: A refresher. IEEE Signal Process. Mag. **21**(1), 112–114 (2004)
39. J.P. Lasalle, *The Stability of Dynamical Systems* (SIAM Press, Philadelphia, 1976)
40. D. Feng, W. Zheng, A. Cichocki, Matrix-group algorithm via improved whitening process for extracting statistically independent sources from array signals. IEEE Trans. Signal Process. **55**(3), 962–977 (2007)
41. M. Steiner, K. Gerlach, Fast converging adaptive processor or a structured covariance matrix. IEEE Trans. Aerosp. Electron. Syst. **36**(4), 1115–1126 (2000)
42. V. Cavo, MCARM/STAP data analysis, Tech Report AFRL-SN-RSTR-1999-48, Vol. 1 (Air Force Research Laboratory, Rome, New York, 1999)